ACS Sustainable Chemistry & Engineering

Research Article

pubs.acs.org/journal/ascecg

Isosorbide-based Polymethacrylates

James J. Gallagher, Marc A. Hillmyer,* and Theresa M. Reineke*

Department of Chemistry, University of Minnesota, 207 Pleasant Street SE, Minneapolis, Minnesota 55455-0431, United States

Supporting Information

ABSTRACT: A new monomer, acetylated methacrylic isosorbide (AMI), was synthesized in two steps employing scandium(III) triflate as a remarkably efficacious catalyst for the tandem esterification of isosorbide with acetic anhydride and methacrylic anhydride. Analysis of the crude product mixture after acetylation indicated that functionalization occurred preferentially at the *endo* hydroxyl group of isosorbide (*endo*-acetate:*exo*-acetate = 4.2:1). Reaction of this mixture with methacrylic anhydride gave the corresponding isomeric mixture of AMI monomers. Poly(AMI) [PAMI] prepared by radical polymerization of the mixture of AMI regioisomers was found to have a high glass transition temperature ($T_g \approx 130$ °C) and good thermal stability (T_d, 5% weight loss; N_2 = 251 °C, air = 217 °C). Reversible addition−fragmentation chain transfer (RAFT) polymerization of AMI using a new chain transfer agent, hydroxyethyl 4-cyano-4-(phenylcarbonothioylthio)pentanoate (HO-CPAD), yielded PAMI-CTA samples with controlled molar masses and narrow molar mass distributions ($Đ \leq 1.09$). Subsequent chain extension of PAMI-CTA with *n*-butyl acrylate gave a series of PAMI-*b*-PnBA block copolymers ranging from 17−36 wt % PAMI. All samples of PAMI-*b*-PnBA exhibited two well-separated T_g values at approximately −45 and +120 °C, indicative of microphase separation.

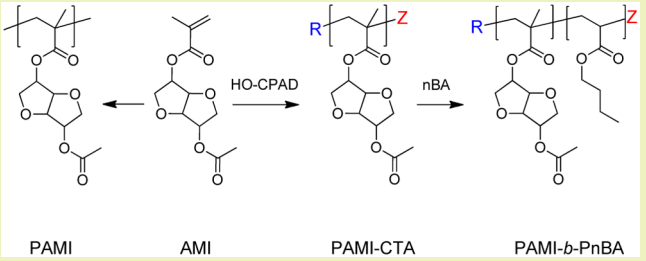

KEYWORDS: *Renewable, polymer, high T_g, RAFT, block copolymer, scandium(III) triflate, butyl acrylate*

INTRODUCTION

Renewable chemical feedstocks are becoming increasingly cost competitive with petroleum based analogs as a result of advances in synthetic methods and production processes. For example, recent improvements in the conversion of the glucose derivative sorbitol to isosorbide have made the latter a viable building block for biobased polymers on the commercial scale.[1,2] Often compared to bisphenol A due to its rigid bicyclic structure and diol functionality, isosorbide has been incorporated into a wide variety of step growth polymers, including polyesters, polycarbonates, polyethers, polyurethanes, and polytriazoles.[3−5] These polymers generally exhibit high glass transition temperatures (T_g) due to the rigid bicyclic structure of isosorbide. Additionally, various difunctional derivatives of isosorbide have been employed in the synthesis of cross-linked, thermoset polymers for use in high performance composites.[6−11]

Despite the numerous examples of isosorbide-based polymers, there are only a few examples of monovinyl isosorbide derivatives for use in linear chain growth polymerizations.[12−15] A monovinyl isosorbide monomer is an appealing building block because the construction of polymers with designed architectures is more easily accomplished via chain growth mechanisms. Beghdadi et al. have described the synthesis and reversible addition−fragmentation chain transfer (RAFT) polymerization of isosorbide derived vinyl dianhydrohexitol triazoles (VDTs).[12] Interestingly, the authors found that the placement of the vinyl triazole moiety at either the *endo* or *exo* position of isosorbide had a significant effect on the solubility and T_g of poly(VDT)s. Polymers prepared from monomer with the vinyl triazole group in the *endo* position had a $T_g \approx 71$ °C and were water-soluble, whereas those prepared from monomer with the vinyl triazole in the *exo* position had a $T_g \approx 118$ °C and were insoluble in water. The authors noted that the RAFT polymerization of VDTs required about 48 h to reach 50−70% conversion, presumably due to the bulky nature of VDT monomers and modest reactivity of the *N*-vinyl triazole moiety.

Various options for functionalizing the hydroxyl groups of isosorbide have been reported in the literature (e.g., esterification, etherification, carbonylation, tosylation).[4] Due to the relatively poor reactivity of the secondary alcohols, esterification methods typically employ the use of auxiliary reactants. For example, a routine procedure for acetylating isosorbide uses acetic acid, *N*,*N*-dicylcohexylcarbodiimide, and catalytic 4-dimethylaminopyridine (i.e., Steglich esterification).[16,17] Acetylation by this method occurs predominantly at the less sterically encumbered *exo* position (~60% of product mixture) due to the steric bulk of the *O*-acyl isourea intermediate (for structure of isosorbide, see Scheme 1). An alternative approach for acetylation uses acetic anhydride and catalytic lead(II) oxide (~2 mol % relative to isosorbide).[18−21] This method favors acetylation at the *endo* position (~80% isolated yield). Although more sterically hindered due to being

Received: December 23, 2014
Revised: February 10, 2015
Published: March 13, 2015

DOI: 10.1021/sc5008362
ACS Sustainable Chem. Eng. 2015, 3, 662−667

Scheme 1. Synthesis of AMI[a]

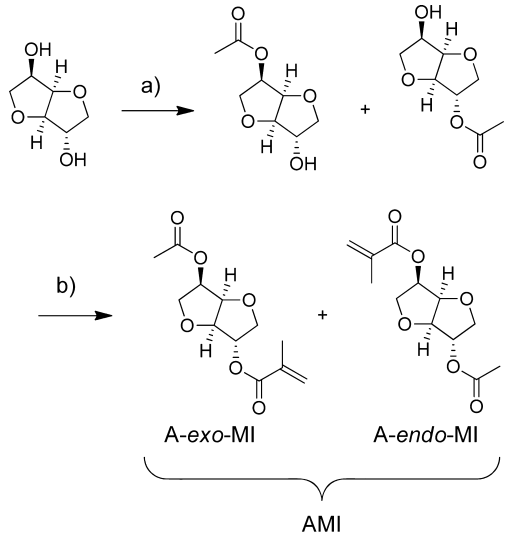

[a](a) 1 mol equiv acetic anhydride, 0.05 mol % $Sc(OTf)_3$, acetonitrile, room temperature, 10 min; (b) 0.97 mol equiv methacrylic anhydride, 1 mol % $Sc(OTf)_3$, acetonitrile, room temperature, 4 h.

on the interior of the puckered bicyclic structure, the alcohol in the *endo* position is more nucleophilic due to intramolecular hydrogen bonding with the ethereal oxygen of the opposite tetrahydrofuran ring.[22] Unfortunately, this strategy requires the use of a toxic heavy metal salt. Likewise, synthesis of methacrylic isosorbide has been reported via Steglich esterification methods,[23] use of methacrylic anhydride and stoichiometric equivalent of an amine base,[6] or methacryloyl chloride and an equivalent of triethylamine.[7] Although these approaches are effective, the use of relatively large amounts of auxiliary reactants is less than ideal from a green chemistry point of view.

In this work, we sought to enable the development of advanced materials such as block copolymers using isosorbide by efficiently synthesizing a new monovinyl isosorbide derivative. To this end, we report the (i) synthesis and characterization of acetylated methacrylic isosorbide (AMI); (ii) use of scandium(III) triflate ($Sc(OTf)_3$) as an active and *endo*-selective esterification catalyst for the functionalization of isosorbide; (iii) polymerization of AMI via conventional free radical polymerization to afford linear high T_g polymers (PAMI); (iv) synthesis and use of a new, efficient hydroxy functional chain transfer agent (HO-CPAD) for the RAFT polymerization of AMI to give PAMI-CTA; (v) synthesis of block copolymer PAMI-*b*-PnBA by chain extension of PAMI-CTA with *n*-butyl acrylate.

RESULTS AND DISCUSSION

Synthesis of AMI. AMI was prepared in two steps according to Scheme 1. In both steps, $Sc(OTf)_3$ was used to catalyze the esterification of isosorbide with the corresponding anhydride. Compared to alternative Lewis acid catalysts, $Sc(OTf)_3$ and other lanthanide triflates have unusual stability toward air and water.[24,25] As a result, they can be handled under ambient atmosphere, do not require anhydrous reaction conditions, and can be easily recycled and reused without loss of activity. Although $Sc(OTf)_3$ is known to be an effective Lewis acid catalyst for the esterification of various alcohols,[26−28] this is the first report, to our knowledge, employing this catalyst for the esterification of isosorbide. Notably, $Bi(OTf)_3$ has also been reported as an effective water tolerant catalyst for the acetylation of isosorbide with acetic anhydride.[29]

In the first step of AMI synthesis, $Sc(OTf)_3$ was found to be an exceptionally active catalyst. Full consumption of acetic anhydride (1 mol eq) occurred in less than 10 min at room temperature using a catalyst loading of 0.05 mol %. By comparison, reported reaction times for acetylation with acetic anhydride and 2 mol % lead(II) oxide range from 2−20 h. Analysis of the crude product mixture by ^{1}H NMR spectroscopy indicated that the *endo* hydroxyl was the preferred site for acetylation ([*endo*-acetate]:[*exo*-acetate] = 4.2:1.0; see Figure S1, Supporting Information).

After isolating the monoacetylated isosorbide products by column chromatography (54% yield), $Sc(OTf)_3$ was again used as a catalyst in the second step to install the methacrylate moiety (Scheme 1b). Complete conversion of methacrylic anhydride (0.97 mol equiv) was reached after 4 h at 1 mol % catalyst loading. The reduced reactivity relative to the first step is attributed to the difference in sterics between acetic anhydride and methacrylic anhydride. Additionally, the majority of hydroxyl groups available for functionalization in the second step are located in the less active (but more sterically accessible) *exo* position ($Sc(OTf)_3$ catalyzed methacrylation of isosorbide with methacrylic anhydride also occurs preferentially at the *endo* position).

To characterize each isomer individually, pure samples of A-*exo*-MI and A-*endo*-MI were prepared by isolating select fractions from column chromatography of the first step containing only isosorbide *endo*-acetate or isosorbide *exo*-acetate, respectively, before installing the methacrylate moiety. Both A-*exo*-MI and A-*endo*-MI were clear viscous liquids at room temperature. Differential scanning calorimetry (DSC) showed identical T_g values for the monomers A-*exo*-MI and A-*endo*-MI at −42 °C, and no evidence for crystallinity was observed for either isomer (Figures S2 and S3, Supporting Information). Fourier transform infrared (FT-IR) spectroscopy showed characteristic peaks at 1740 and 1717 cm^{-1} corresponding to the acyl and methacrylate esters, respectively, and the C=C bond stretch of the methacrylate group was apparent at 1637 cm^{-1} (Figures S4 and S5, Supporting Information). Other than subtle differences at low wavenumbers, no significant difference was observed in the FT-IR spectra for A-*exo*-MI and A-*endo*-MI. ^{1}H NMR spectra differed significantly between A-*exo*-MI and A-*endo*-MI due to the different arrangement of substituents about the isosorbide core (Figures S6 and S7, Supporting Information). Of particular note is the difference in chemical shift observed for the vinyl protons *cis* to the carbonyl oxygen (Figure 1). Additional structural confirmation was provided by high resolution mass spectrometry of the 4:1 mixture of A-*exo*-MI:A-*endo*-MI (expected, 256.2518; found, 279.0839 ($M + Na^+$); error 4.63 ppm). Overall, AMI was readily prepared as a mixture of isomers in two steps from isosorbide on a ∼20 g scale with a final (unoptimized) overall yield of 44%. The use of low catalyst loadings, mild reaction conditions, and inexpensive commercially available reagents make this synthetic pathway appealing for potential large scale production of this new monomer.

Free Radical Polymerization of AMI. Thermally initiated free radical polymerization of AMI (4:1 A-*exo*-MI:A-*endo*-MI) was carried out in the presence of azobis(isobutyronitrile) (AIBN) at 70 °C in $CHCl_3$. Aliquots taken during the

DOI: 10.1021/sc5008362
ACS Sustainable Chem. Eng. 2015, 3, 662−667

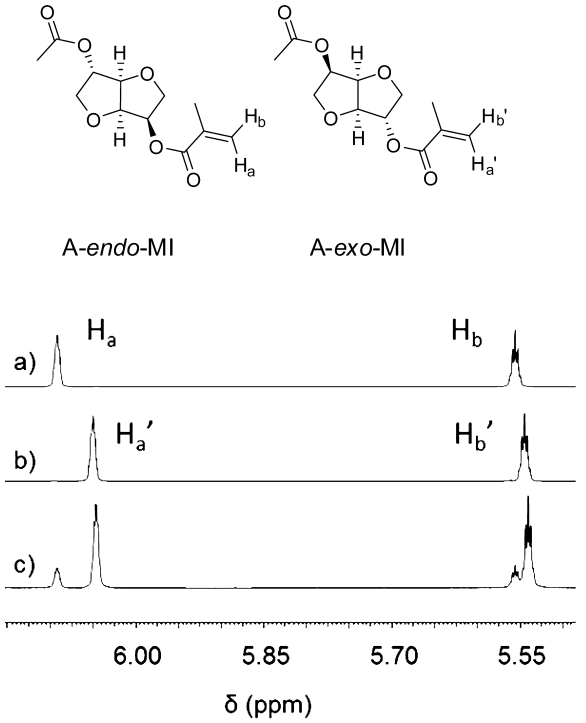

Figure 1. ^{1}H NMR spectra in $CDCl_3$ of the vinyl region for (a) A-*endo*-MI, (b) A-*exo*-MI, and (c) 4:1 mixture of A-*exo*-MI:A-*endo*-MI.

polymerization were analyzed by ^{1}H NMR spectroscopy to determine conversion as a function of time (Figure S8, Supporting Information). ^{1}H NMR analysis indicated 83% monomer conversion after 4 h. Monitoring the relative integrations of resonances corresponding to H_a and H_a' (Figure 1) indicated no significant difference in reactivity between A-*endo*-MI and A-*exo*-MI. After precipitation and drying, this sample of PAMI was soluble at 10 wt % in acetone, EtOAc, CH_2Cl_2, $CHCl_3$, THF, and DMF but was insoluble in water, MeOH, iPrOH, and toluene. The number-average molar mass (M_n) of this sample by size exclusion chromatography in THF with multiangle laser light scattering detection (SEC-MALLS) was 88.9 kg mol^{-1} with $Đ$ = 1.80 (Figure S9, Supporting Information). Thermogravimetric analysis (TGA) showed a T_d (5% weight loss) of 251 and 217 °C under N_2 and air, respectively (Figures S10 and S11, Supporting Information). Similar values of T_d (~230 °C) under inert atmosphere have been reported previously for poly(methyl methacrylate) (PMMA) prepared by free radical polymerization.[30] Under air, this sample of PAMI was stable for ~20 min at 180 °C (<1% weight loss, Figure S12, Supporting Information). The sample exhibited a remarkably high T_g of 130 °C by DSC (Figure S15, Supporting Information). Because the T_g of PMMA is ~110 °C,[31] the relatively high T_g of PAMI is attributed to reduced polymer flexibility caused by additional steric bulk of the pendant isosorbide acetate groups.

To determine the effect of stereochemistry on polymer thermal properties, an isomerically pure sample of PAMI was prepared from A-*endo*-MI under the same conditions described above. Similarly, after 4 h at 70 °C, the polymerization of A-*endo*-MI reached 84% conversion, as determined by ^{1}H NMR spectroscopy. M_n and $Đ$ of PA-*endo*-MI by SEC-MALLS analysis were 105 kg mol^{-1} and 1.48, respectively (Figure S14, Supporting Information). TGA and DSC revealed no significant difference in T_d or T_g between PAMI and PA-*endo*-MI, indicating that the regiochemistry of substituents on isosorbide does not alter the thermal properties of PAMI (Table S1, Figures S15−17, Supporting Information). Based on these results, AMI and PAMI can be prepared without the need for careful consideration of isomer composition in the final product. By contrast, Beghdadi et al. reported that regiochemistry had a significant impact on the T_g of poly(VDT)s.[12] A key difference between the reported poly(VDT)s and PAMI is the absence of hydroxyl groups in the latter, suggesting that these groups, if left unprotected, play an important role in determining polymer properties.

PAMI-CTA via RAFT polymerization. Controlled radical polymerization allows for the synthesis of macromolecules with well-defined architectures.[32−35] Block copolymers, which find use in many applications such as thermoplastic elastomers, pressure sensitive adhesives, and toughening agents,[36] are readily prepared by controlled radical polymerization methods. The thermal stability and high T_g of PAMI make it a promising sustainable candidate for a hard component of a block copolymer system.[37] To demonstrate the ability to incorporate PAMI into a block copolymer, AMI was prepared via RAFT polymerization to give PAMI-CTA (Scheme 2a). An initial

Scheme 2. Synthesis of (a) PAMI-CTA, [HO-CPAD]:[AIBN] = 10:1, 70 °C, 18 h; (b) PAMI-*b*-PnBA, [*n*-butyl acrylate]:[PAMI-CTA]:[AIBN] = 870:1:0.1, 70 °C, 20 h[a]

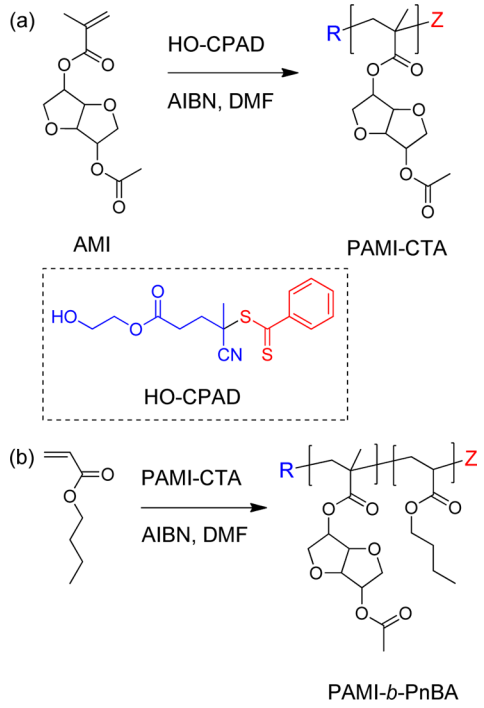

[a]Z and R correspond to the dithiobenzoate and free radical leaving group fragments, respectively, of HO-CPAD.

screening showed that dithiobenzoates were the most suitable class of chain transfer agent (CTA) for RAFT polymerization of AMI, whereas trithiocarbonates did not result in well controlled polymerizations (Table S2, Supporting Information). The CTA that afforded the highest monomer conversion while maintaining low $Đ$ of the resultant polymer was 4-cyano-4-(phenylcarbonothioylthio)pentanoate (HO-CPAD). This new CTA, a structural analogue of the previously reported CTA 4-cyano-1-hydroxypent-4-yl dithiobenzoate,[38] was synthe-

DOI: 10.1021/sc5008362
ACS Sustainable Chem. Eng. 2015, 3, 662−667

sized by Steglich esterification of the commercially available 4-cyano-4-(phenylcarbonothioylthio)pentanoic acid with excess ethylene glycol (Scheme S1, Supporting Information). After purification by column chromatography, HO-CPAD was isolated in a 67% yield. Use of HO-CPAD as a RAFT CTA results in functional polymers with a hydroxyl end group (Scheme 2), a particularly useful structural motif given the synthetic versatility of a hydroxyl group (e.g., in the preparation of block copolymers containing mechanistically differentiated components). A linear increase in M_n with conversion and narrow molecular weight distribution indicated the RAFT polymerization of AMI with HO-CPAD was well controlled (Figure 2). However, the linear fit to the M_n vs conversion data

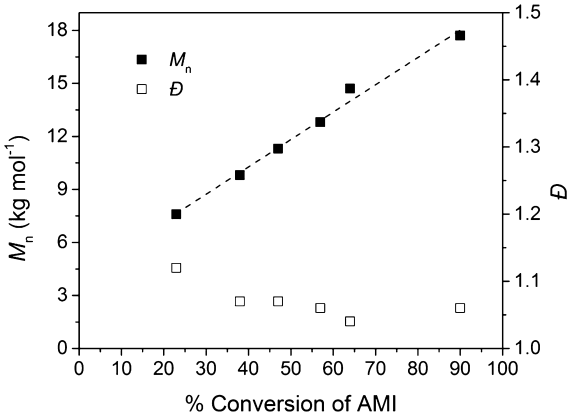

Figure 2. M_n and $Đ$ as a function of conversion for RAFT polymerization of AMI. [AMI]:[HO-CPAD]:[AIBN] = 60:1:0.1. Conversion determined by ^{1}H NMR spectroscopy; M_n and $Đ$ determined by SEC-MALLS in THF. Dashed line indicates a linear regression, R^2 = 0.99.

has a nonzero intercept. This phenomenon can be attributed to non-RAFT propagation events occurring at low conversion before the main RAFT equilibrium has been established.[39]

Because a key advantage of controlled radical polymerization is the ability to synthesize materials with targeted molar masses and narrow distributions, AMI was polymerized by RAFT employing different ratios of $[AMI]_0$:$[HO\text{-}CPAD]_0$ (Table 1). In all cases, the polymerization proceeded to >92% conversion after 18 h and $Đ$ < 1.09 was achieved for all samples. Analysis of PAMI-CTA (14) by ^{1}H NMR spectroscopy confirmed the presence of the expected end groups (Figure S18, Supporting Information). Resonances between 7.36 and 7.89 ppm correspond to the aromatic protons of the dithiobenzoate group, whereas a peak at 4.23 ppm corresponds to the protons α to the alcohol of the free radical leaving group fragment. Further proof of a terminal hydroxyl group was demonstrated by reacting PAMI-CTA (14) with a 10-fold excess of methacrylic anhydride in the presence of $Sc(OTf)_3$ (14 mol % relative to polymer) to give ene-PAMI-CTA (14) (Scheme S2, Supporting Information). Again, $Sc(OTf)_3$ was found to be an efficacious esterification catalyst. After 1 h of reaction at room temperature followed by repeated precipitation into MeOH and drying under vacuum, ene-PAMI-CTA (14) was isolated as a pink powder. The disappearance of the peak at 4.23 ppm along with the appearance of a new peak at 4.36 ppm confirmed the terminal hydroxyl group was fully functionalized, while resonances corresponding to the methacrylic protons were observed in the vinyl region at 5.62 and 6.14 ppm (Figure S19, Supporting Information).

Values of M_n, as determined by ^{1}H NMR end group analysis (assuming one CTA fragment per chain) and SEC-MALLS, were in reasonably good agreement, although the values determined by SEC-MALLS were consistently higher (see Table 1). Values of M_n (calc.)/M_n (SEC) were < 1 for all trials, indicating a deviation from the ideal one CTA per chain model (i.e, CTA efficiency factor < 1).[40] For comparison, the M_n (calc.)/M_n (NMR) values were consistently closer to 1. Because conversions and M_n (calc.)/M_n (SEC) and M_n (calc.)/M_n (NMR) were consistent across all trials, PAMI-CTA of a targeted M_n can be reliably synthesized by RAFT using HO-CPAD.

PAMI-CTA (14) exhibited similar thermal stability under N_2 and air (T_d = 255 and 252 °C, respectively, Figures S20 and S21, Supporting Information). T_g values of PAMI-CTA ranged from 91 to 108 °C depending on M_n of the sample (Figure S22, Supporting Information). From the linear regression of T_g vs 1/M_n data based on the Flory–Fox equation, T_g becomes essentially constant at 130 °C for PAMI at molar masses > 55 kg mol^{-1} (Figure S23, Supporting Information). These predicted values are in good agreement with the T_g values observed for PAMI and PA-*endo*-MI prepared by conventional free radical polymerization.

PAMI-*b*-PnBA. Chain extension of PAMI-CTA with *n*-butyl acrylate afforded the block copolymer samples PAMI-*b*-PnBA (Scheme 2b, Table 1). PnBA is an appealing option for a rubbery counterpart to PAMI due to its low T_g (~−50 °C)[31] and recent developments toward the commercial production of

Table 1. PAMI-CTA and PAMI-*b*-PnBA Sample Information

sample	$[M]_0/[CTA]_0$	conv. (%)[a]	M_n (NMR) (kg mol^{-1})[b]	M_n (SEC) (kg mol^{-1})[c]	M_n (calc.) (kg mol^{-1})[d]	M_n (calc.)/M_n (SEC)	M_n (calc.)/M_n (NMR)	$Đ$[c]
PAMI-CTA (14)	40	95	11.8	13.8	10.1	0.73	0.86	1.07
PAMI-CTA (17)	50	95	15.0	16.7	12.5	0.75	0.83	1.06
PAMI-CTA (19)	60	95	16.9	18.7	14.9	0.80	0.88	1.09
PAMI-CTA (24)	80	92	21.7	24.2	19.2	0.79	0.88	1.07
PAMI-CTA (31)	100	92	28.1	30.9	23.9	0.77	0.85	1.08
PAMI-*b*-PnBA (14–69)	870	64	82.7	88.3	85.1	0.96	1.03	1.12
PAMI-*b*-PnBA (17–55)	870	51	71.8	70.7	73.5	1.04	1.02	1.12
PAMI-*b*-PnBA (19–60)	870	56	78.6	85.7	81.1	0.95	1.03	1.19
PAMI-*b*-PnBA (24–54)	870	50	80.3	78.7	79.9	1.01	1.00	1.14
PAMI-*b*-PnBA (31–56)	870	52	87.1	102	88.8	0.87	1.02	1.24

[a]Of monomer, determined by ^{1}H NMR spectroscopy. [b]From end group analysis. [c]Determined by SEC-MALLS in THF. [d]Assuming each CTA generates 1 polymer chain (see the Supporting Information).

DOI: 10.1021/sc5008362
ACS Sustainable Chem. Eng. 2015, 3, 662–667

biobased acrylates.[41] In all cases, the PAMI-*b*-PnBA samples had a broader molar distribution relative to that of PAMI-CTA. Inspection of the SEC traces showed a small high molar mass shoulder, likely due to termination by combination of propagating radicals (Figures 3 and S24–27, Supporting Information). Termination events are deviations from ideal behavior for controlled radical polymerizations and result in broadened molar mass distributions. TGA of PAMI-*b*-PnBA showed marked increase in T_d compared to PAMI-CTA (14) homopolymer (T_d, 5% weight loss; N_2 = 316 °C, air = 296 °C, Figures S28 and S29, Supporting Information). The higher T_d of PAMI-*b*-PnBA compared to PAMI is due to the differences in thermal stability and decomposition mechanisms between poly(acrylate)s and poly(methacrylate)s. Poly(acrylate)s undergo thermal decomposition by a random-chain scission mechanism with a T_d ~310 °C,[42] whereas poly(methacrylate)s typically decompose by an end-chain mechanism at relatively lower temperatures.[43] For PAMI-CTA, methacrylic chain ends are likely generated by *in situ* thermolysis of the CTA end group during TGA.[44] Therefore, the relatively higher thermal stability of PAMI-*b*-PnBA is attributed to the absence of methacrylic chain ends. All samples of PAMI-*b*-PnBA exhibited two well-separated T_g values at approximately −45 and +120 °C (Figure S30, Supporting Information). The presence of both T_g's near that of the respective homopolymers suggests the PAMI and PnBA domains are microphase separated, an essential feature for thermoplastic elastomer applications.

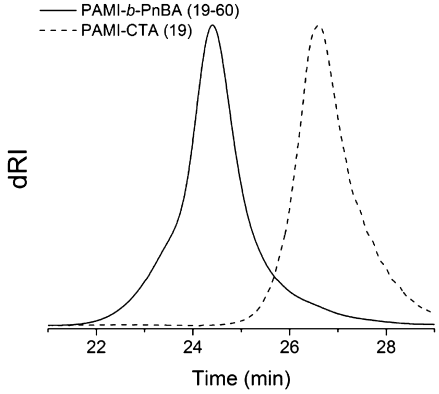

Figure 3. THF-SEC of PAMI-*b*-PnBA (19–60) and PAMI-CTA (19) prepared by RAFT polymerization.

CONCLUSION

In summary, we have reported the synthesis of a new isosorbide derived monomer AMI in two steps from commercially available starting materials. $Sc(OTf)_3$ was employed in both steps as a highly active Lewis acid catalyst for the esterification of isosorbide with anhydrides. PAMI prepared by free radical polymerization was found to have a high T_g and similar thermal stability relative to PMMA. Comparison of PAMI and PA-*endo*-MI demonstrated that the regiochemistry of AMI was not a determining factor for polymer thermal properties. AMI was successfully polymerized via RAFT using the novel CTA HO-CPAD to afford PAMI-CTA with good control of M_n and narrow $Đ$. Esterification of the hydroxyl end group of PAMI-CTA with methacrylic anhydride yielded ene-PAMI-CTA, further demonstrating the utility of $Sc(OTf)_3$ as a Lewis acid catalyst. PAMI-CTA was subsequently chain extended with *n*-butyl acrylate to give the block copolymer PAMI-*b*-PnBA. Combined, these advances have tremendous potential for the valorization of biobased and low cost isosorbide. Additional research focusing on thermoplastic elastomer applications for PAMI containing block copolymers is ongoing.

ASSOCIATED CONTENT

Supporting Information

Additional information as noted in text. This material is available free of charge via the Internet at http://pubs.acs.org.

AUTHOR INFORMATION

Corresponding Authors

*M. A. Hillmyer. E-mail: hillmyer@umn.edu.
*T. M. Reineke. E-mail: treineke@umn.edu.

Notes

The authors declare no competing financial interest.

ACKNOWLEDGMENTS

This work was supported by the NSF under the Center for Sustainable Polymers, CHE-1413862. The authors thank Lidia Swanson for her general laboratory assistance and Jeff Ting and Debbie Schneiderman for their help with preparing this paper.

REFERENCES

(1) Zhang, J.; Li, J.; Wu, S.-B.; Liu, Y. Advances in the catalytic production and utilization of sorbitol. *Ind. Eng. Chem. Res.* **2013**, *52*, 11799–11815.
(2) Scott, A. Roquette embraces biobased materials. *C&EN* **2014**, *90*, 16–17.
(3) Fenouillot, F.; Rousseau, A.; Colomines, G.; Saint-Loup, R.; Pascault, J. P. Polymers from renewable 1,4:3,6-dianhydrohexitols (isosorbide, isomannide and isoidide): A review. *Prog. Polym. Sci.* **2010**, *35*, 578–622.
(4) Rose, M.; Palkovits, R. Isosorbide as a renewable platform chemical for versatile applications—Quo vadis? *ChemSusChem* **2012**, *5*, 167–176.
(5) Besset, C.; Pascault, J.-P.; Fleury, E.; Drockenmuller, E.; Bernard, J. Structure-properties relationship of biosourced stereocontrolled polytriazoles from click chemistry step growth polymerization of diazide and dialkyne dianhydrohexitols. *Biomacromolecules* **2010**, *11*, 2797–2803.
(6) Shin, S.; Kim, B. C.; Chang, E.; Cho, J. K.; Suh, D. H. A biobased photocurable binder for composites with transparency and thermal stability from biomass-derived isosorbide. *RSC Adv.* **2014**, *4*, 6226–6231.
(7) Sadler, J. M.; Nguyen, A. P. T.; Toulan, F. R.; Szabo, J. P.; Palmese, G. R.; Scheck, C.; Lutgen, S.; La Scala, J. J. Isosorbide-methacrylate as a bio-based low viscosity resin for high performance thermosetting applications. *J. Mater. Chem. A* **2013**, *1*, 12579–12586.
(8) Ge, J.; Trujillo, M.; Stansbury, J. Synthesis and photo-polymerization of low shrinkage methacrylate monomers containing bulky substituent groups. *Dent. Mater.* **2005**, *21*, 1163–1169.
(9) Pion, F.; Reano, A. F.; Ducrot, P.-H.; Allais, F. Chemo-enzymatic preparation of new bio-based bis- and trisphenols: New versatile building blocks for polymer chemistry. *RSC Adv.* **2013**, *3*, 8988–8997.
(10) Feng, X.; East, A. J.; Hammond, W. B.; Zhang, Y.; Jaffe, M. Overview of advances in sugar-based polymers. *Polym. Adv. Technol.* **2011**, *22*, 139–150.
(11) Besset, C.; Bernard, J.; Fleury, E.; Pascault, J. P.; Cassagnau, P.; Drockenmuller, E.; Williams, R. J. J. Bio-sourced networks from thermal polyaddition of a starch-derived α-azide-ω-alkyne AB monomer with an A2B2 aliphatic cross-linker. *Macromolecules* **2010**, *43*, 5672–5678.
(12) Beghdadi, S.; Miladi, I. A.; Ben Romdhane, H.; Bernard, J.; Drockenmuller, E. RAFT polymerization of bio-based 1-vinyl-4-

DOI: 10.1021/sc5008362
ACS Sustainable Chem. Eng. 2015, 3, 662–667

dianhydrohexitol-1,2,3-triazole stereoisomers obtained via click chemistry. *Biomacromolecules* **2012**, *13*, 4138−4145.
(13) Mansoori, Y.; Hemmati, S.; Eghbali, P.; Zamanloo, M. R.; Imanzadeh, G. Nanocomposite materials based on isosorbide methacrylate/CLOISITE 20A. *Polym. Int.* **2013**, *62*, 280−288.
(14) Koyama, H.; Tsutsumi, K. Polymerizable monomer polymeric compound resin compositions for photoresist and method for producing semiconductor. World Patent WO 2004113404 A1, December 29, 2004.
(15) Sato, K.; Kodama, K. Positive-working far-UV photoresists. Japan Patent JP 2004341062 A, December 1, 2004.
(16) Cekovic, Z.; Tokic, Z. Selective esterification of 1,4:3,6-dianhydro-D-glucitol. *Synthesis* **1989**, *1989*, 610−612.
(17) Shaikh, A. L.; Kale, A. S.; Shaikh, M. A.; Puranik, V. G.; Deshmukh, A. R. A. S. Asymmetric synthesis of β-lactams by [2+2] cycloaddition using 1,4:3,6-dianhydro-D-glucitol (isosorbide) derived chiral pools. *Tetrahedron* **2007**, *63*, 3380−3388.
(18) Stoss, P.; Merrath, P.; Schlüter, G. Regioselektive acylierung von 1,4:3,6-dianhydro-D-glucit. *Synthesis* **1987**, *1987*, 174−176.
(19) Berini, C.; Lavergne, A.; Molinier, V.; Capet, F.; Deniau, E.; Aubry, J.-M. Iodoetherification of isosorbide-derived glycals: Access to a variety of O-alkyl or O-aryl isosorbide derivatives. *Eur. J. Org. Chem.* **2013**, *2013*, 1937−1949.
(20) Abenhaïm, D.; Loupy, A.; Munnier, L.; Tamion, R.; Marsais, F.; Quéguiner, G. Selective alkylations of 1,4:3,6-dianhydro-D-glucitol (isosorbide). *Carbohydr. Res.* **1994**, *261*, 255−266.
(21) Van Buu, O. N.; Aupoix, A.; Hong, N. D. T.; Vo-Thanh, G. Chiral ionic liquids derived from isosorbide: Synthesis, properties and applications in asymmetric synthesis. *New J. Chem.* **2009**, *33*, 2060−2072.
(22) Lemieux, R.; McInnes, A. The preferential tosylation of the endo-5-hydroxyl group of 1,4; 3,6-dianhydro-D-glucitol. *Can. J. Chem.* **1960**, *38*, 136−140.
(23) Xu, M.; Wang, W.; Xia, L.; Lin, G. Development of a new reaction system for the synthesis of highly optically active α, γ-substituted γ-butyrolactones. *J. Org. Chem.* **2001**, *66*, 3953−3962.
(24) Kobayashi, S.; Sugiura, M. Rare-earth metal triflates in organic synthesis. *Chem. Rev.* **2002**, *102*, 2227−2302.
(25) Kobayashi, S. Scandium triflate in organic synthesis. *Eur. J. Org. Chem.* **1999**, 15−27.
(26) Ishihara, K.; Kubota, M.; Kurihara, H.; Yamamoto, H. Scandium trifluoromethanesulfonate as an extremely active acylation catalyst. *J. Am. Chem. Soc.* **1995**, *117*, 4413−4414.
(27) Ishihara, K.; Kubota, M. Scandium trifluoromethanesulfonate as an extremely active Lewis acid catalyst in acylation of alcohols with acid anhydrides and mixed anhydrides. *J. Org. Chem.* **1996**, *3263*, 4560−4567.
(28) Barrett, A.; Braddock, D. C. Scandium(III) or lanthanide(III) triflates as recyclable catalysts for the direct acetylation of alcohols with acetic acid. *Chem. Commun.* **1997**, *10*, 351−352.
(29) Howard, S.; Hagberg, E.; Rockafellow, E. Method for quantitative analysis of sugars, sugar alcohols and related dehydration products. U.S. Patent US 20130337570 A1, December 19, 2013.
(30) Ferriol, M.; Gentilhomme, A.; Cochez, M.; Oget, N.; Mieloszynski, J. L. Thermal degradation of poly(methyl methacrylate) (PMMA): Modelling of DTG and TG curves. *Polym. Degrad. Stab.* **2003**, *79*, 271−281.
(31) Brandrup, J.; Immergut, E.; Grulke, E.; Abe, A.; Bloch, D. *Polymer handbook*, 4th ed.; 1999; Vol. *49*.
(32) Gregory, A.; Stenzel, M. H. Complex polymer architectures via RAFT polymerization: From fundamental process to extending the scope using click chemistry and nature's building blocks. *Prog. Polym. Sci.* **2012**, *37*, 38−105.
(33) Boyer, C.; Stenzel, M.; Davis, T. Building nanostructures using RAFT polymerization. *J. Polym. Sci., Part A: Polym. Chem.* **2011**, *49*, 551−595.
(34) Moad, G.; Rizzardo, E.; Thang, S. H. Living radical polymerization by the RAFT process - A third update. *Aust. J. Chem.* **2012**, *65*, 985.
(35) Matyjaszewski, K. Atom transfer radical polymerization (ATRP): Current status and future perspectives. *Macromolecules* **2012**, *45*, 4015−4039.
(36) Bates, F. S.; Fredrickson, G. H. Block copolymers—Designer soft materials. *Phys. Today* **1999**, *52*, 32−38.
(37) Holmberg, A. L.; Reno, K. H.; Wool, R. P.; Epps Iii, T. H. Biobased building blocks for the rational design of renewable block polymers. *Soft Matter* **2014**, *10*, 7405−7424.
(38) Chong, Y.; Krstina, J.; Le, T.; Moad, G. Thiocarbonylthio compounds in free radical polymerization with reversible addition-fragmentation chain transfer (RAFT polymerization). Role of the free-radical leaving group (R). *Macromolecules* **2003**, *60*, 2256−2272.
(39) Favier, A.; Charreyre, M.; Chaumont, P.; Pichot, C. Study of the RAFT polymerization of a water-soluble bisubstituted acrylamide derivative. 1. Influence of the dithioester structure. *Macromolecules* **2002**, *35*, 8271−8280.
(40) Favier, A.; Charreyre, M.-T. Experimental requirements for an efficient control of free-radical polymerizations via the reversible addition-fragmentation chain transfer (RAFT) process. *Macromol. Rapid Commun.* **2006**, *27*, 653−692.
(41) Tullo, A. H. Hunting For biobased acrylic acid. *Chem. Eng. News* **2013**, *91*, 18−19.
(42) Liufu, S.-C.; Xiao, H.-N.; Li, Y.-P. Thermal analysis and degradation mechanism of polyacrylate/ZnO nanocomposites. *Polym. Degrad. Stab.* **2005**, *87*, 103−110.
(43) Beyler, C. L.; Hirschler, M. M. Thermal decomposition of polymers. In *SFPE Handbook of Fire Protection Engineering*; DiNenno, P. J., Ed.; National Fire Protection Association: Quincy, MA, 2001; pp 110−131.
(44) Willcock, H.; O'Reilly, R. K. End group removal and modification of RAFT polymers. *Polym. Chem.* **2010**, *1*, 149−157.

DOI: 10.1021/sc5008362
ACS Sustainable Chem. Eng. 2015, 3, 662−667